

# Determination of Carrier-Transfer Length from Side-Wall Quantum Well to Quantum Wire by Micro-Photoluminescence Scanning

Z.-F. LI,<sup>1,4</sup> W. LU,<sup>1</sup> X.-Q. LIU,<sup>1</sup> X.-S. CHEN,<sup>1</sup> S.C. SHEN,<sup>1</sup> Y. FU,<sup>2</sup>  
M. WILLANDER,<sup>2</sup> H.H. TAN,<sup>3</sup> and C. JAGADISH<sup>3</sup>

1.—National Laboratory for Infrared Physics, Shanghai Institute of Technical Physics, Chinese Academy of Sciences, Shanghai 200083, China. 2.—Physical Electronics and Photonics, Microelectronic Center at Chalmers, Department of Microelectronics and Nanoscience, Chalmers University of Technology, S-412 96 Göteborg, Sweden. 3.—Department of Electronic Material Engineering, Research School of Physical Science and Engineering, the Australian National University, Canberra 0200, A.C.T., Australia. 4.—E-mail: zfli@mail.sitp.ac.cn

Micro-photoluminescence ( $\mu$ -PL) line scanning across a single V-groove, GaAs/AlGaAs quantum wire (QWR) has been performed at room temperature, revealing a clear spatial-dependence of the PL. After fitting each PL spectrum by multi-Gaussian line shapes, intensity profiles of each PL component from confined structures have been obtained as functions of the scanning position. The PL quenching of a side-wall quantum well (SQWL) has been recognized in a certain area in the vicinity of the QWR and is interpreted by carrier transfer into the QWR within effective transfer length. By simulating the carrier-transfer process from SQWL to QWR as a convolution of a step function for carrier distribution and a Gaussian function for exciting laser irradiance, the effective transfer length of about  $1.8 \pm 0.3 \mu\text{m}$  has, therefore, been concluded.

**Key words:** V-groove quantum wire, carrier-transfer length, micro-photoluminescence

## INTRODUCTION

In comparing bulk and two-dimensional semiconductors, one-dimensional quantum wire (QWR) (one dimension is extended and the other two dimensions are confined) has an energy density of states consisting of discrete peaks at sublevel energies. It has been demonstrated recently in V-groove QWRs that a population inversion is obtained at a lower threshold current in QWR lasers.<sup>1,2</sup> In such devices, the efficient carrier trapping into the QWR region is essential because of the small active volume in QWR lasers.<sup>3</sup> The side-wall quantum well (SQWL) could be a good channel through which carriers inject into QWR. In practical applications, however, top quantum well (TQWL) and a certain part of SQWL should be electrically degraded in order to form current-blocking regions to reduce dark and threshold currents and to suppress parasitic-recombination centers.<sup>4</sup> The optimization of laser performance,

therefore, requires a compromise between extending the carrier capturing/injecting channel by increasing the area of the SQWL neighboring the QWR and reducing the carrier-escaping channel by decreasing the area of the SQWL neighboring the TQWL. The balance would be established by retaining the QWR-neighbored SQWL to be as large as possible within the effective carrier-transferring length and eliminating the other parts. In this sense, the effective carrier-transfer length becomes crucial in determining the area of the SQWL to be retained. Carrier-transfer processes in cleaved-edge overgrown QWRs have been studied by R.D. Grober et al. using near-field scanning-optical microscopy.<sup>5</sup> However, for V-groove QWR, the information of carrier transfer is insufficient. In this article, we report a micro-photoluminescence ( $\mu$ -PL) line-scanning study of GaAs/AlGaAs QWR structures at room temperature. By using a small excitation-laser spot and the same small PL-collecting diaphragm, the effective carrier-transfer length is deduced from the  $\mu$ -PL scanning over QWR and SQWL regions.

(Received August 25, 2002; accepted February 25, 2003)

## EXPERIMENTAL

The V-groove QWR sample was grown by metal-organic vapor-phase epitaxy. Before growth, a GaAs (100) semi-insulating substrate was patterned using contact lithography processes and wet etching. The pattern consisted of 50 stripes 2- $\mu\text{m}$  wide with 2- $\mu\text{m}$  spacing. After pattern transfer, the wafer was etched in an  $\text{H}_3\text{PO}_4\text{:H}_2\text{O}_2\text{:H}_2\text{O}$  solution (1:1:3) at  $0^\circ\text{C}$  to form a V-groove surface profile (about 2.5- $\mu\text{m}$  in depth). The V grooves were aligned along the [011] direction. Then, the substrate was cleaned with warm trichloroethylene, acetone, and methanol. Finally, before being loaded into the growth chamber, the substrate was trimly etched with  $\text{H}_2\text{SO}_4\text{:H}_2\text{O}_2\text{:H}_2\text{O}$  (20:1:1) for 20 sec. A 0.1- $\mu\text{m}$  GaAs-buffer layer was grown before a 1- $\mu\text{m}$   $\text{Al}_{0.5}\text{Ga}_{0.5}\text{As}$  bottom-barrier layer. A nominal 1-nm GaAs-well layer was then deposited followed by a 0.1- $\mu\text{m}$   $\text{Al}_{0.5}\text{Ga}_{0.5}\text{As}$  top-barrier layer. Finally, a 200-nm GaAs-cap layer was grown. All layers were undoped, and the growth temperature was  $750^\circ\text{C}$ . More detailed sample preparation and geometric parameters can be found in Ref. 6. Figure 1 shows the schematic cross section of the quantum structures of such a V-groove QWR system together with a schematic diagram of the  $\mu\text{-PL}$  line scanning. The  $\mu\text{-PL}$  scanning was carried out on a Jobin Yvon LabRam-INFINITY micro-Raman (Lille, France) spectrometer with the excitation of the 514.5-nm line of an  $\text{Ar}^+$  laser. With a  $\times 100$  microscope objective (NA = 0.90), the laser beam was focused to about 0.8  $\mu\text{m}$  in diameter, which was determined by the scanning-intensity profile of the Si-Raman peak of  $520\text{ cm}^{-1}$  across an Al-covered interface.<sup>7</sup> The illuminating power is about  $80\text{ kW/cm}^2$  on the sample surface. To prevent any possible luminescence from regions other than the illuminated spot to get into the spectrometer, the entrance diaphragm of the spectrometer was set to be 50  $\mu\text{m}$  in diameter, which

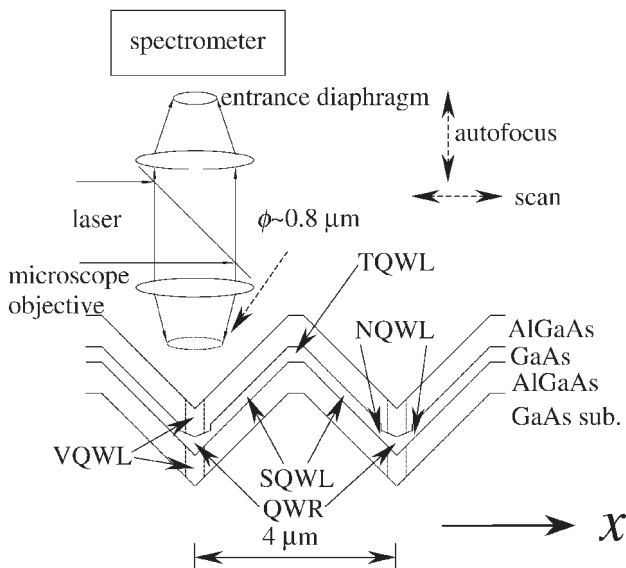


Fig. 1. The geometric structure of V-groove QWRs and the schematic diagram of the  $\mu\text{-PL}$  line scanning.

equals the image size of the laser spot and enables the probed-PL light to come only from the region located at the illuminated spot and be confined to about 0.8  $\mu\text{m}$  in diameter. The line-scanning direction was along the x-axis with an advancing step of 0.1  $\mu\text{m}$ . There was a piezoelectric-ceramic adjuster mounted between the objective and the mounting turret, which allows variation of the z position of the objective. Before each exposure at each step, a quick z scanning of this adjuster, in combination with signal-automated analysis and feedback control, allows the detection of the surface for each measurement point to achieve auto focus.

## RESULTS AND DISCUSSION

Figure 2 shows the complete PL-spectrum profile recorded by the line scanning. It consists of a central-valley area (where the QWR is located) and two peaked areas at the two sides of the central valley, showing clear spatial dependence of the PL. Typical PL spectra in these different areas are illustrated in Fig. 3 at (a) 1  $\mu\text{m}$  left to the center, (b) V-groove center, and (c) 1  $\mu\text{m}$  right to the center. Spectrum (a) and (c) are the first two spectra showing strong peaks at about 1.939 eV, when the exciting/collecting spot is moving away from the QWR. Although in Fig. 3a there are still some remnants of the PL at 1.743 eV, the spectrum is dominated by the PL at 1.939 eV. The lowest energy peak at 1.422 eV is from bulk GaAs. The highest energy peak at 2.066 eV corresponds to the transition between the X valley in the conduction band and the  $\Gamma$  point in the valence band of the  $\text{Al}_{0.5}\text{Ga}_{0.5}\text{As}$  barrier, which has an indirect-bandgap structure. The PL peaks between 1.422 eV and 2.066 eV come from various confined-quantum structures. According to the theoretical analysis<sup>8</sup> and the sample structure,<sup>6,8</sup> these PL peaks are attributed to QWR (1.743 eV), SQWL (1.939 eV), necking quantum well (NQWL, 1.967 eV), vertical quantum well (VQWL, 1.886 eV), and TQWL (1.865 eV), respectively, as labeled in Fig. 3. The VQWL is low Al-fraction AlGaAs well layers formed by the migration of Ga atoms to the bottom of the V-groove during the growth of AlGaAs

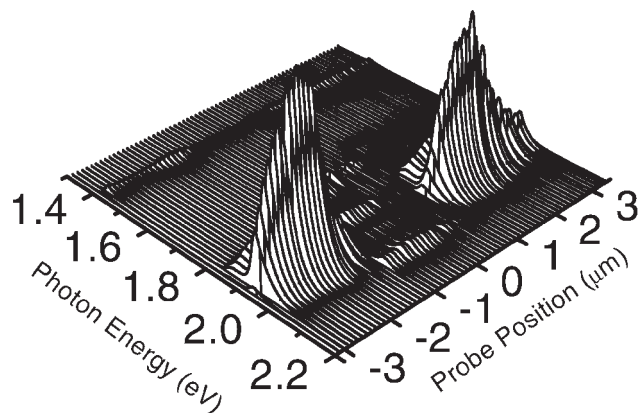


Fig. 2. The  $\mu\text{-PL}$  spectra versus position. The spatial dependence of the PL spectra is clearly shown.

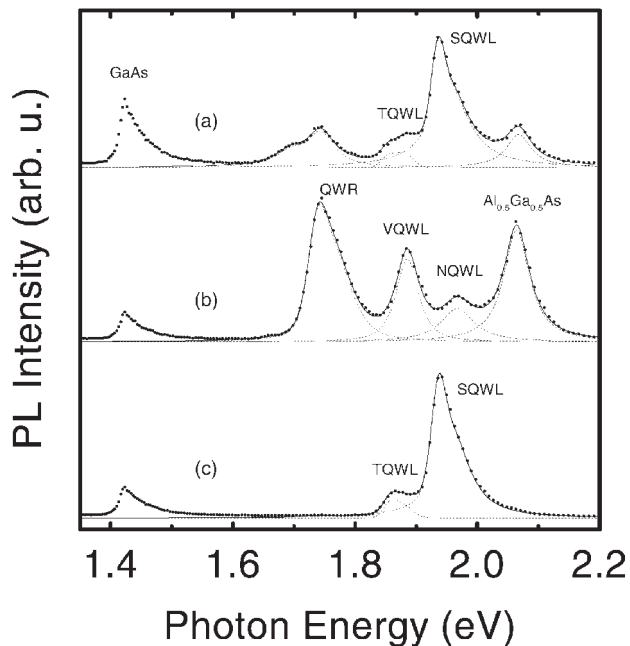


Fig. 3. The PL spectra from V-groove quantum structures at different positions: (a) 1  $\mu\text{m}$  left to the QWR, (b) center of the QWR, and (c) 1  $\mu\text{m}$  right to the QWR. The dotted curves are the experimental data, and the dashed lines are obtained by the asymmetric data-fitting technique described in Ref. 7. The solid lines are the combination of each PL component.

because of the larger mobility of Ga than that of Al atoms.<sup>6</sup>

To realize the position dependence of the PL characteristics, each of the acquired spectra has been peak-fitted. Because of the asymmetric nature of the PL peaks in line shape,<sup>9</sup> an asymmetric-Gaussian line shape<sup>7</sup> has been employed to fit each PL component in the experiment curve. The dashed lines in Fig. 3 represent the decomposed components, while the solid lines are for the fitted curves. The fitting meets the experimental dots very well. Then, the integrated intensity of each PL component is extracted. Figure 4 shows the PL-intensity profile against the spatial position for the QWR and the SQWL, where the position of the QWR is referred as  $x = 0 \mu\text{m}$ . Here, it is clearly seen that the QWR PL is the strongest at  $x = 0 \mu\text{m}$ , while it decreases when the position moves away from the center. The profile line shape of the QWR-PL intensity is slightly asymmetric because of the structural asymmetry in the sample.

A prominent phenomenon in Fig. 4 is that no SQWL PL occurred in the QWR-PL dominating region, which is consistent with Fig. 2. The peak intensity of the SQWL PL is only observed at about  $1.5 \mu\text{m} \leq |x| \leq 2.5 \mu\text{m}$ , where the laser spot is about over the top of the V-groove.

Why does the SQWL quench its PL in the area near the QWR while it is always illuminated (the lateral dimension of the QWR is only about 30 nm,<sup>6</sup> and the exciting-laser spot is about 0.8  $\mu\text{m}$  in diameter)? We try to interpret this behavior with the following dynamic process. The optical absorption

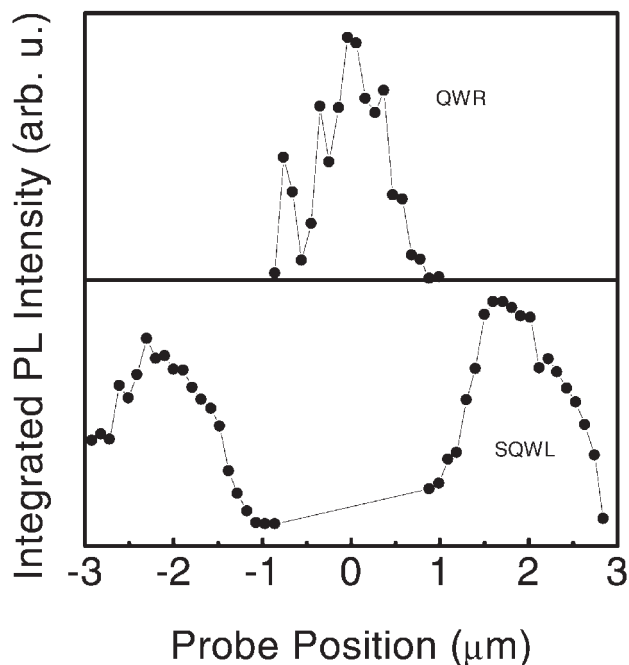


Fig. 4. The integrated intensities of QWR and SQWL PL peaks as functions of the illumination/detection position.

occurs mostly in the AlGaAs-barrier layer because of its large spatial volume. Photogenerated carriers diffuse into either the SQWL or the VQWL, where the energy level is relatively lower. As the transition energy of the QWR is about 196 meV and 143 meV smaller than that of the SQWL and VQWL, respectively, the carriers will further transfer into the QWR within their effective transfer length and lifetime, where they recombine to emit light. Therefore, the PL of the SQWL is mainly determined by the carriers staying in the SQWL. Here, we propose a critical, effective carrier-transfer length,  $l_D$ . When the free carrier is away from the QWR at a distance larger than  $l_D$ , it will stay in the SQWL. Otherwise, the carrier will be captured by the QWR and has no contribution to the PL of the SQWL. Although an exponential distribution of the carrier density is expected by the diffusion equation, the built-in electric-field-assisted dynamic process near the QWR helps trap the carriers by the QWR before their radiative recombination. So that as long as the carriers are excited in the near-QWR region within the distance of  $l_D$ , the carriers will be almost completely trapped by the QWR before they recombine. When the carriers are excited beyond the distance of  $l_D$ , the diffusion equation determined carrier distribution along the SQWL will give the PL profile of the SQWL. Considering this carrier-dynamic process and in our weak excitation condition, the PL intensity of the SQWL,  $I(x)$ , will be proportional to the carrier density staying in the SQWL and can be expressed as a step function:

$$I(x) = 0 \quad \text{for } |x - x_R| \leq l_D$$

$$I(x) = 1 \quad \text{for } |x - x_R| > l_D$$

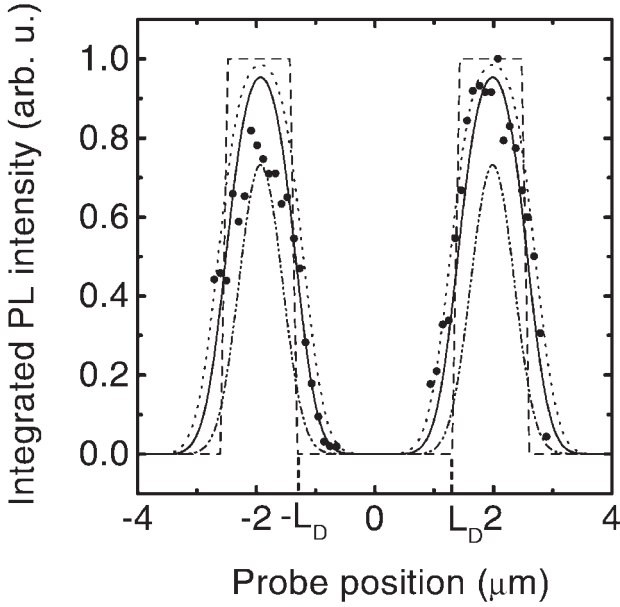


Fig. 5. The calculated SQWL PL-intensity profile (solid line) against position by the convolution of a Gaussian function and a step function. The solid dots are the experimental data. The dashed line is the step function by taking the critical effective carrier-transfer length  $l_D = 1.3 \mu\text{m}$  and the period value of  $4 \mu\text{m}$ . The dashed line and the dash-dotted line are for  $l_D = 1.1 \mu\text{m}$  and  $1.5 \mu\text{m}$ , respectively. Therefore,  $l_D$  is concluded to be  $1.3 \pm 0.2 \mu\text{m}$ .

where  $x$  is the axis perpendicular to both the material growth and QWR directions, as indicated in Fig. 1. The  $x_R$  is the position of the QWR on the  $x$ -axis. This function is shown in Fig. 5 by the dashed line by assuming  $l_D = 1.3 \mu\text{m}$ . As the QWRs are separated from each other with the period of  $4 \mu\text{m}$  in our sample, the  $I(x)$  also shows such a  $4\text{-}\mu\text{m}$  periodicity.

Because the exciting-laser beam distributes its energy in Gaussian profile, the carrier density and, therefore, the PL intensity is determined by the convolution of the  $I(x)$  and the Gaussian function,  $i(x)$ :

$$\text{PL}(x) = \int I(x') i(x - x') dx'$$

where  $i(x)$  is experimentally determined to be

$$i(x) = \exp[-(x - x_L)^2/0.8^2]$$

where  $x_L$  is the center position of the laser spot. By taking  $l_D$  as  $1.3 \mu\text{m}$ , the calculated PL-intensity dependence of the SQWL on the lateral position is shown in Fig. 5 in the solid line, which is in good agreement with the experimental data in dots. Also shown in Fig. 5 are the other two calculated curves in dotted and dash-dotted lines with  $l_D = 1.1 \mu\text{m}$  and  $1.5 \mu\text{m}$ , respectively. One can see that all the experimental data are included within the area between these two lines. As a result, we conclude the value of  $l_D$  to be  $1.3 \pm 0.2 \mu\text{m}$  in the measured sample.

When taking the geometric parameters into account, the effective carrier-transfer length from the SQWL to the QWR becomes  $l_D/\sin 45^\circ = 1.8 \pm 0.3 \mu\text{m}$  because  $l_D$  is along the  $x$ -axis and is angled with the SQWL in  $45^\circ$ .

## CONCLUSIONS

In conclusion,  $\mu$ -PL line scanning has been performed on a single V-groove GaAs/AlGaAs QWR at room temperature, by which PL spectra from various quantum structures have been recorded. In the area of the QWR, the dominant PL peaks are from QWR, VQWL, and NQWL at the energies of  $1.743 \text{ eV}$ ,  $1.886 \text{ eV}$ , and  $1.967 \text{ eV}$ , respectively. At the position of about  $1 \mu\text{m}$  away from the QWR, the SQWL PL starts its domination at  $1.939 \text{ eV}$ . The fitted-PL intensity versus the scanning position for each luminescent component reveals the origins of the PL signals. The quenching of the SQWL PL in the vicinity of the QWR is interpreted by the carrier-transferring effect. By deconvoluting the PL-intensity profile with a Gaussian function and a step function, the length of the photo-excited carrier transfer from SQWL into QWR is determined to be about  $1.8 \pm 0.3 \mu\text{m}$  in our measured sample. This is expected to be an important parameter in the design and optimization of QWR devices.

## ACKNOWLEDGEMENTS

This work was supported by the State Key Program of China No. G1998061404, the Australian Agency for International Development through IDP Education Australia under Australia-China Institutional Links Program, and the National Natural Science Foundation of China Nos. 10074068, 60244002, and 10234040. X.-S. Chen thanks the financial support of the "One-hundred-person project" of the Chinese Academy of Sciences.

## REFERENCES

1. E. Kapon, D.M. Hwang, and R. Bhat, *Phys. Rev. Lett.* **63**, 430 (1989).
2. S. Tiwari, G.D. Petit, K.R. Milkove, F. Legoues, R.J. Davis, and J.M. Woodall, *Appl. Phys. Lett.* **64**, 3536 (1994).
3. C. Kiener, L. Rota, A.C. Maciel, J.M. Freylan, and J.F. Ryan, *Appl. Phys. Lett.* **68**, 2061 (1996).
4. C. Percival, P.A. Houston, J. Woodhead, M. Al-Khafaji, G. Hill, J.S. Roberts, and A.P. Knights, *IEEE Trans. Electron Dev.* **ED-47**, 1769 (2000).
5. R.D. Grober, T.D. Harris, J.K. Trautman, E. Betzig, W. Wegscheider, L. Pfeiffer, and K. West, *Appl. Phys. Lett.* **64**, 1421 (1994).
6. X.Q. Liu et al., *Appl. Phys. Lett.* **75**, 3339 (1999).
7. E. Cresson, ed., *Raman and Luminescence Spectroscopy for Microelectronics* (Luxembourg: Office for Official Publications of the European Communities, 1998), pp. 92–94.
8. Y. Fu, M. Willander, X.Q. Liu, W. Lu, S.C. Shen, H.H. Tan, S. Yuan, and C. Jagadish, *Superlattices Microstr.* **26**, 307 (1999).
9. Y. Fu, M. Willander, Z.F. Li, and W. Lu, *J. Appl. Phys.* **89**, 5112 (2001).